Proceedings of the ASME 2024
International Design Engineering Technical Conferences and
Computers and Information in Engineering Conference
IDETC-CIE2024
August 25-28, 2024, Washington, DC

DETC2024-142947

DESIGN AND FABRICATION OF A DEPLOYABLE TENSEGRITY MILLIROBOT FOR NEXT-GENERATION GASTROINTESTINAL DIAGNOSTICS AND TREATMENT

Christian Kazoleas[1, *], Jiajun Zhang[1, *], Na Tan[2, †], Sichen Yuan[1, ‡]

[1] The University of Alabama, Tuscaloosa, AL, 35487
[2] Lawrence Technological University, Southfield, MI, 48075

ABSTRACT

The advent of robotics in medicine has brought about a paradigm shift, enabling minimally invasive interventions for in-vivo practices. Pill-based robots, specifically designed at the millimeter scale, have emerged as a viable alternative to traditional endoscopic methods for gastrointestinal tract diagnostics and treatment. These millirobots, capable of navigating the complex and constrained environments of the human body, offer a significant advantage by enabling thorough visualization or targeted drug delivery in a single session without the need for sedation. We previously developed a novel deployable tensegrity robot, designed for gastrointestinal diagnostics and treatment, which addresses the limitations of conventional capsule endoscopes through its unique structure and locomotion mechanism. Tensegrity structures, characterized by a network of components in tension and compression, provide an innovative solution to the challenges of designing robots for in-vivo applications. Our millimeter-scale tensegrity robot leverages the inherent advantages of such structures—lightweight, high stiffness, and adaptability—to navigate through densely packed tissues and high-pressure environments within the GI tract. Inspired by the locomotion of earthworms, the movement mechanism of the robot enables efficient navigation and precise positioning, significantly reducing the risk of retention and ensuring patient safety. This paper investigates the design and fabrication process of the tensegrity robot, focusing on achieving a high folding ratio to facilitate its deployment as a pill-based robot. Through a comparison of the robot's fabricated dimensions with the theoretical design, we evaluate the accuracy of the fabrication process, highlighting the potential of this innovative approach in transforming GI tract diagnostics and treatment. The deployment of such tensegrity-based millirobots marks a new era in medical devices, promising enhanced patient safety and comfort through non-invasive methods.

1. INTRODUCTION

With the rapid advancements in robotics and autonomy, millimeter-scale robots have shown significant potential for minimally invasive operations. These millirobots operate within the human body by collecting critical health diagnostics and administering therapeutic drugs without causing discomfort to the patient [1]. Examples of millirobots include pilled-based robots [2-3], designed to the dimensions of a swallowable pill capsule and introduced into the body non-invasively via ingestion. These pill-based robots consist of a hard shell-like outer skin and use small propellers to navigate the digestive system while collecting data, delivering drugs, and performing minimally invasive operations [4]. Therefore, these millirobots can replace the traditional invasive endoscope as a diagnostic approach and treatment for gastrointestinal (GI) tract diseases, such as GI bleeding and celiac disease. Similarly, these robotic systems facilitate both active and passive modalities of medical intervention, enabling the identification of issues with the capacity for direct treatment in a single sedation-free session [5].

While millirobots can significantly improve the comfort and safety of the patient, the main requirement for these robots is safety due to operational use inside the human body. This is an important concern since the development of these millirobots still faces substantial challenges in structural design and

[*] Graduate student, Department of Aerospace Engineering and Mechanics.
[†] Graduate student, A. Leon Linton Department of Mechanical, Robotics and Industrial Engineering.
[‡] Assistant Professor, Department of Aerospace Engineering and Mechanics, sichen.yuan@ua.edu.

locomotion mechanisms. The primary risks associated with millirobots stem from the potential failure of their movement mechanisms and retention in the internal tracts of the human body. Thus, to ensure reliability in operation, the millirobot must have a simple and reliable approach for morphing and an effective locomotion mechanism that ensures an exit from confined areas [6, 7]. Hard-body millirobots are more likely to become lodged or stuck in narrow spaces, as their inflexible bodies hinder their ability to adapt and morph within constrained environments [8-10]. In comparison, soft-bodied robots address this issue by increasing the flexibility [11-14]. However, these robots rely on fragile joints as their primary locomotion mechanism. This reliance complicates achieving high operational reliability, a critical factor for successful in-vivo applications. The challenge is further heightened in high-pressure environments, such as densely packed tissues, where these millirobots must navigate safely and efficiently. Consequently, a millirobot with a rigid yet flexible body, which can provide consistent locomotion regardless of the environmental conditions, is needed.

A tensegrity-based approach is a viable solution that addresses the structural design and locomotion mechanisms issues afflicting current millirobots. A tensegrity structure is a pin-jointed structure composed of isolated members in compression (usually bars or struts) inside a net of continuous members in tension (usually cables or tendons). The main advantage of using a tensegrity-based solution is its ability to maintain a desired shape without complex joints or mechanisms, which can be found in origami-based deployable structures [15, 16]. Thus, a tensegrity-based approach leverages lightweight and high-stiffness characteristics to help provide structural integrity while in high-pressure environments. Similarly, the tensegrity-based approach provides a simple locomotion mechanism by changing the length of the cables, allowing the millirobot to navigate through the GI tract and densely packed tissues without retention. While modern tensegrity robots have shown great promise in adapting to new environments and have proved to be an effective solution in the macroscale for accomplishing various tasks [17-24], these robots require miniaturization to the millimeter scale to ensure compatibility with the spatial constraints of the human body.

This paper proposes the design and fabrication of a deployable tensegrity robot on the millimeter scale for gastrointestinal diagnostics and treatment. The highlight of the deployable tensegrity millirobot is the flexible, yet rigid body achieved from the tensegrity-based approach and the incorporation of the locomotion mechanism that is inspired by the crawling movement of earthworms, enabling it to move effectively within confined spaces using Shape Memory Alloy (SMA). This novel design is anticipated to significantly reduce the risk of retention within the narrow and winding pathways of the GI tract while facilitating swift navigation and precise positioning. In addition, this paper will investigate the folded length and various dimensions of the fabricated robot compared to the theoretical design. This comparison will help quantify the accuracy of the fabrication process through percentage error evaluation and allow for specific identification of improvement during the manufacturing process. Understanding these differences will enable the refinement of design specifications to ensure reliability while operating inside the human body. While also providing valuable insights into the practical challenges of miniaturizing tensegrity-based robots. Overall, the innovative design and fabrication of the deployable tensegrity millirobot will help significantly enhance patient safety and comfort for GI diagnostics and treatment.

2. PROTOTYPE DESIGN AND LOCOMOTION

2.1 Topology Design and Form Finding

The overall topology design of a tensegrity-based robot helps define the number of nodes and their respective cable members. Applying these parameters with various form-finding techniques, such as Force Density Method, Dynamic Relaxation Method, and Stochastic Fixed Nodal Position Method (SFNPM), allows for obtaining an optimal geometric configuration [25-29]. From previous results [30,31], the topology used for a unit cell of the proposed millirobot will form the shape of an icosahedron, as shown in Fig. 1. The newly deployed diameter and length of the unit cell are 9 and 8 millimeters (mm), respectively. When folded, the diameter increases to 10 mm, and the length drastically decreases to 1.5 mm.

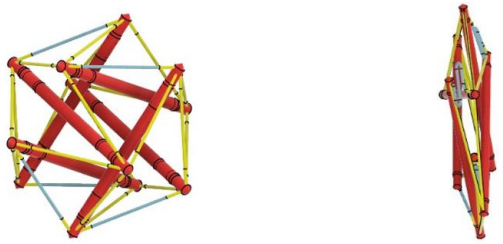

(a) (b)

FIGURE 1: (a) SINGLE DEPLOYED ICOSAHEDRON UNIT CELL, (b) SINGLE FOLDED ICOSAHEDRON UNIT CELL

The individual bar members are duplicates of each other to help ensure a quick production time. The length of the bar member is 8.5 mm, with a cross-sectional area of 0.25 mm^2. The bar material is stainless steel, and the elastic cable network material is a Thermoplastic Polyurethane (TPU) called Ninjaflex. The length of a cable member from one node to the next is 4.25 mm and has a cross-sectional area of 0.08 mm^2. The entire body of the tensegrity-based millirobot, shown in Fig. 2, is composed of three six-bar member unit cells, with the dimensions of a complete body listed in Table 1. The use of class-1 tensegrity structure allows for the connection of each unit cell without needing a complex mechanism for the connecting bars members. In addition, the diameter of the robot remains consistent regardless of how many unit cells are used, allowing for independent morphing sections. The length of the body is 24 mm during deployment, and when folded, the adjusted length is 4.5 mm. Thus, the body of the millirobot can fold to 18.75 percent of the fully deployed length, giving the robot a high folding ratio.

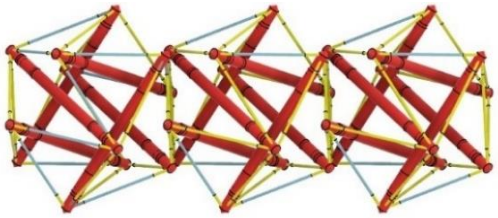

FIGURE 2: COMPLETE BODY OF THE TENSEGRITY-BASED MILLIROBOT

TABLE 1: DIMENSIONS OF THE BODY

Component	*Length Deployed (mm)*	*Length Folded (mm)*	*Diameter Deployed (mm)*	*Diameter Folded (mm)*
Singular Unit Cell	8.0	1.5	9.0	10.0
Complete Body	24.0	4.5	9.0	10.0

2.2 Actuation

The crawling motion of an earthworm inspires the locomotion mechanism for the deployable tensegrity millirobot. This is achieved by placing active cables in the system to decrease the cable length between various nodes. As illustrated in Figs. 1 and 2, the system incorporates two types of cables: the elastic passive cables (yellow) fabricated by TPU, and the active cables (blue), composed of SMA actuators. The choice of SMA actuators for the active cables is due to its property of undergoing a transformation in response to thermal stimuli. This characteristic enables the SMA actuator incorporated cables to revert to a predetermined shape upon the application of external energy, effectively acting as the muscle of the robot. Activation of these cables induces the robot to assume a compact and folded configuration. Removal of the thermal stimulus allows the robot to deploy by the stored potential energy within the elastic passive cables, thus returning the robot to its original deployed state.

2.3 Skin Design

A soft outer layer acting as the skin of the deployable millirobot is applied to help ensure ease of swallowing and protection in the human body, as shown in Fig. 3. The outer skin prevents the structural components of the robot, such as bar members and sharp edges, from causing harm to the internal tissues in the human body by accidental pinching or cutting. Beyond its protective capabilities, the over-layering skin is vital in optimizing movement through the GI tract. This enhances the efficiency of the robot and minimizes the risk of tissue irritation or damage during the procedure. The design of the skin considers the need for durability and flexibility by incorporating a sequence of ribs that ensures a high reliability during use. Similarly, the thickness of the skin is 0.8 mm, with the material being Formlabs Elastic Resin 50A. The dimension of the millirobot with the skin is shown in Table 2. When folded, the length of the robot is 7.5 mm, and when deployed, it is 33 mm. Similarly, the diameter of this millirobot is 10.8 mm when folded and 9.8 mm when deployed. Thus, the deployable millirobot can fold to 22.72 percent of its deployed length inside the human body, meaning adding skin still promotes a high folding ratio.

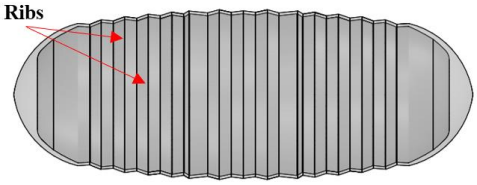

FIGURE 3: CROSS SECTION OF PROPOSED SKIN FOR THE TENSEGRITY-BASED MILLIROBOT

TABLE 2: DIMENSIONS OF MILLIROBOT

Component	*Length Deployed (mm)*	*Length Folded (mm)*	*Diameter Deployed (mm)*	*Diameter Folded (mm)*
Without Skin	24.0	4.5	9.0	10.0
With Skin	33.0	7.5	9.8	10.8

2.4 Locomotion Plan Inside the GI Tract

The main goal in creating a new deployable tensegrity-based millirobot is to combine flexibility with rigidity, enabling it to navigate the GI tract reliably. Therefore, the millirobot is designed to travel the intestines, maintaining a folded configuration as it moves through the system. Upon necessity for altering its orientation, dislodging from entrapments, or administering medication, the robot activates its biomimetic locomotion, which resembles the movement of an earthworm, as detailed in Fig. 4. The movement process of the millirobot initiates from the first phase, a folded state. In the second phase, disengaging active cable members at the front enables the advancement of the millirobot. This results in the expansion and narrowing of the front unit cells, powered by the natural potential energy from the elastic passive cable members. This action increases the pressure at the forefront of the robot, propelling it forward. When the expansion is complete, the millirobot goes into the third phase, the transition, where the front active cables are re-energized. Subsequently, the contraction of these active cable members reduces the size of the middle unit cell, effectively drawing the rear of the robot forward in Phase 3. To ensure a seamless transition, the active cables at the posterior of the robot extend, allowing the rear unit cells to expand as they are pulled forward, culminating in Phase 4. The millirobot then reverts to its compact form; this cycle of phases is repeated, enabling it to achieve a continuous forward crawl when needed.

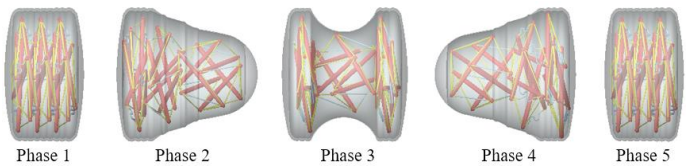

FIGURE 4: DIAGRAM OF THE MILLIROBOTS BIOMIMICKING MOVEMENT INSIDE OF THE HUMAN BODY

3. PROTOTYPE FABRICATION

3.1 Overview and Equipment

The millimeter design concept outlined in the previous section has yet to be implemented in the actual world. Therefore, a thorough fabrication process is required. This section presents a millimeter-scale prototype that excludes SMA for actuation. A basic outline of the fabrication process for the millirobot is depicted in Fig. 5. The process involves manual assembly without the use of complicated techniques or special equipment.

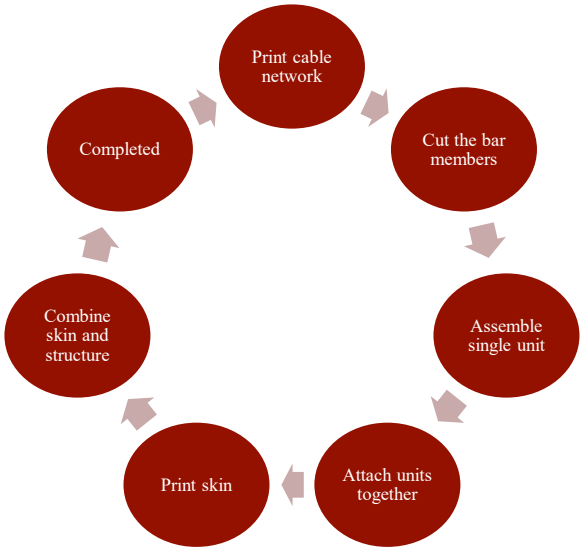

FIGURE 5: PROCESS OF FABRICATING THE MILLIROBOT FROM START TO FINSH

3.2 Cable Network and Bar Members

The first step is to 3D print the cable network using the Prusa MK3+ with the 1.75-mm Ninjaflex filament, which is a type of Thermoplastic polyurethane (TPU) with high elongation percentage before breaking. Ninjaflex can stretch up to 660 percent of its original length. Figure 6 shows the printed cable network and a singular bar on a centimeter grid. The cable network has a thickness of 0.2 mm and is printed with a layer height of 0.1 mm. This means the cable network is only two layers, which could be an issue if the printer experiences under-extrusion during the print. Thus, a top surface ironing feature was included at the end of the print, allowing the printer nozzle to heat up to 238 degrees Celsius and retrace the path slowly to ensure the layers are combined. It can also be noted that the cable network is printed flat on the print bed instead of in a 3D cylinder shape. This provides a simple print without support material, which could cause the cable members to have uneven tension after the post-processing.

The structural components of the millirobot, specifically the bar members, were initially designed to be stainless steel due to its strength and durability. However, considering the scale of these components, a shift was made towards utilizing gold-plated brass pins. These pins, trimmed to a length of 8.5 mm, were selected for their cost and ease of availability. Incorporating metal bar members increases the structural rigidity of the millirobot, enhancing its performance and resilience.

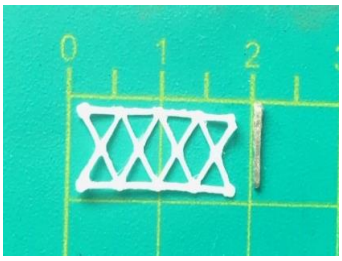

FIGURE 6: NINJAFLEX CABLE NETWORK AND SINGLE BAR USED FOR THE MILLIROBOT ON A CENTIMETER GRID

3.3 Assembly of Single Unit Cell and Attachment

For the assembly of a single unit cell of the millirobot, a singular cable network is printed, accompanied by six metal bar members cut to specifications. The entire assembly of the robot requires the fabrication of three cable networks and a total of eighteen bar members. With the components prepared, the assembly process for a single unit cell begins with shaping the cable network into a cylindrical form. A small adhesive application is added to the connection nodes, ensuring a secure bond. These connection nodes are at the top and bottom and on the furthest left and right nodes of the cable network. The process involves wrapping the top node on the far right around to connect with the rear of the far-left node. This technique is repeated for the bottom connection node. The application of adhesive at these connections ensures their strength, allowing for the initial incorporation of the first two bar members, as demonstrated in Fig. 7(a).

After allowing fifteen minutes for the adhesive to cure, the next phase involves attaching another pair of bar members to two free nodes. This step is performed with an application of adhesive, ensuring each bar is aligned correctly and secured, as shown in Fig. 7(b). During this stage, using tweezers and clamps helps ease the fabrication process. This procedure is repeated until all six bars are integrated with the cable network. Once the adhesive is fully cured for all six fixed-sided bar members, the subsequent phase involves applying a small amount of adhesive to the free end of each bar. This free end is aligned and connected with the corresponding cable node. As previously mentioned, each bar naturally retains its position at this location due to being in an equilibrium state. After this step is repeated for each bar member, a millimeter-scale tensegrity icosahedron unit is fabricated, as shown in Figs. 7(c), and 7(d). This entire process is repeated two more times to get three single structures.

After successfully assembling three individual unit cells, the subsequent phase integrates them into a cohesive structure. The connection points can be determined using advanced form-finding techniques and, in this case, are collected from the previous results [31]. Unlike the conventional triangular faces of an icosahedron tensegrity structure, the designated connection sites are configured to accommodate three additional nodes, forming a hexagon that brings the new nodes into a state of equilibrium. When these nodes are aligned, they seamlessly

integrate into the cable network, resulting in a unified structure. To enhance reliability of the assembly, an adhesive is introduced at the connection points. This additional step ensures the integrity of the millirobot, which is fully assembled and illustrated in Fig. 7(e). Through this process, the millirobot transitions from individual components to a singular, rigid, yet flexible body.

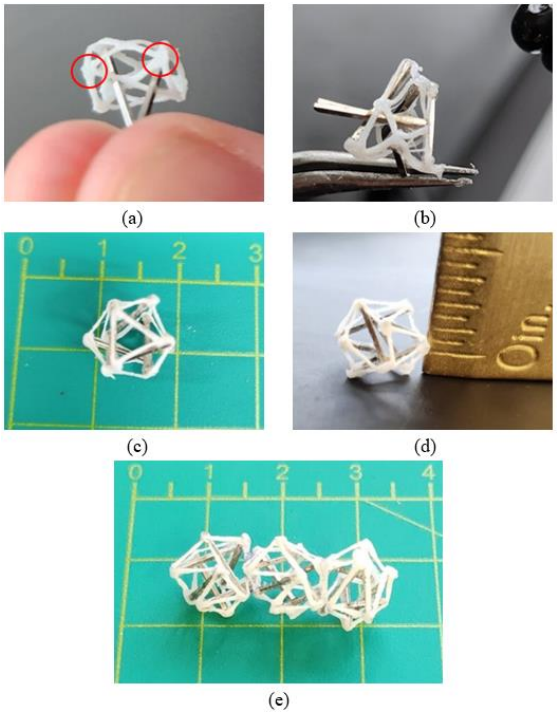

FIGURE 7: (a) CYLINDRICAL NINJAFLEX CABLE NETWORK FORM WITH TWO BAR MEMBERS AND CONNECTING NODES CIRCLED IN RED, (b) NINJAFLEX CABLE NETWORK METHOD FOR CONNECTING MULTIPLE BARS MEMBERS, (c) FABRICATED SINGLE TENSEGRITY UNIT ON A CENTIMETER GRID AS PERSPECTIVE, (d) FABRICATED SINGLE TENSEGRITY UNIT FRONT VIEW WITH AN INCH RULER AS PERSPECTIVE, (e) FABRICATED TENSEGRITY MILLIROBOT BODY ON A CENTIMETER GRID

3.4 Outer Skin and Attachment

The last step in constructing the millirobot is the fabrication and attachment of the outer skin. This component is 3D printed using a Formlabs 3+ SLA printer, utilizing Elastic 50A Resin V2. The design involves printing the skin in two dome-shaped halves, as illustrated in Fig. 8(a), with a wall thickness of 0.8 mm. This design simplifies the attachment process and printing process. Printing the skin in two halves promotes ease of manufacture and ensures that, upon assembly, the skin can be effortlessly aligned and bonded to the robot. Similarly, it allows for a snug fit over the robot without overstretching the material or compressing the robot in multiple directions during fitment. Completing this fabrication process results in a fully assembled millirobot, encapsulated in a protective and flexible skin, displayed in Fig. 8(b).

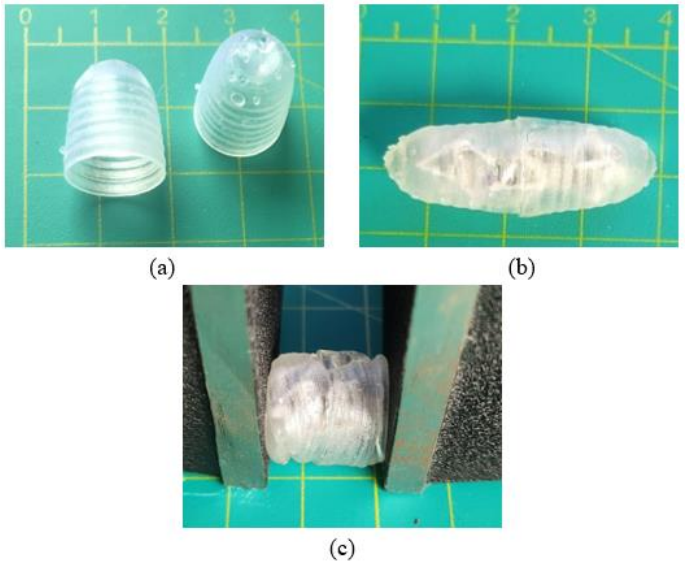

FIGURE 8: (a) FABRICATED ELASTIC 50A RESIN V2 PREPROCESS CAPSULE SKIN, (b) FABRICATED COMPLETED DEPLOYABLE TENSEGRITY MILLIROBOT ON A CENTIMETER GRID, (c) FOLDED TENSEGRITY MILLIROBOT

4. Fabricated Millirobot Results

As illustrated in Fig. 8(b), the deployable tensegrity millirobot has been assembled, yet without including SMA actuators. The integration of actuation and locomotion mechanisms will be addressed in future work. Currently, the fabricated millirobot in a deployed state has a measured length of 34.37 mm, with a diameter of 12.69 mm. Without the actuators, the folded state will need to be measured by positioning the millirobot between two fixed blocks, a process depicted in Fig. 8(c).

When equipped with its skin, the millirobot achieves a folded length of 14.27 mm and a diameter of 13.92 mm, reducing to 41.51 percent of its fully extended length. In contrast, the dimensions of the millirobot without its skin revealed a deployed length of 25.23 mm and a folded length of 6.97 mm. The diameter of the skinless robot measures 9.46 mm when deployed, expanding to 10.37 mm in its folded state. Thus, without attaching the skin, the base millirobot can fold to 27.44 percent of its deployed length. This comparative analysis between the fabricated deployable tensegrity millirobot without and with its skin against the designed specifications is detailed in Tables 3 and 4, respectively.

A significant challenge encountered after the fabrication process was the reduction in the folded length of the millirobot. A likely reason for this issue is inconsistencies in cutting the bar members to the length of 8.5 mm. Any deviation from uniformity might cause the bar members to alter the geometry while compressing slightly, which could obstruct each other. Thus, this issue prevents the millirobot from folding completely flat. Therefore, future fabrication techniques of this millirobot will prioritize that all bar members are cut to precisely the same length, forcing a strict tolerance level. Addressing this issue is

expected to reduce the overall error margin in the body of the robot to approximately five or less percent across all metrics.

TABLE 3: COMPARISON OF FABRICATED AND DESIGNED MILLIROBOT WITHOUT ATTACHED SKIN

Component	*Length Deployed (mm)*	*Length Folded (mm)*	*Diameter Deployed (mm)*	*Diameter Folded (mm)*
Designed Millirobot	24.00	4.50	9.00	10.00
Fabricated Millirobot	25.23	6.97	9.46	10.37
Percent Error	5.12 %	54.88 %	5.11 %	3.70 %

TABLE 4: COMPARISON OF FABRICATED AND DESIGNED MILLIROBOT WITH ATTACHED SKIN

Component	*Length Deployed (mm)*	*Length Folded (mm)*	*Diameter Deployed (mm)*	*Diameter Folded (mm)*
Designed Millirobot	33.00	8.50	9.80	10.80
Fabricated Millirobot	34.37	14.27	12.69	13.92
Percent Error	4.15 %	67.88 %	29.48 %	28.88 %

Applying a skin layer to the robot, as depicted in Table 4, dramatically increases the percentage error in most categories. While the length of the millirobot with the attached skin maintained a low percentage error, the diameters in both the folded and deployed states displayed similarly high error margins. The fabricated millirobots diameter, measured at the thickest point, indicates that the slight overlap where the two halves join could be a source of error. Additionally, applying extra resin at the seam ensuring a water-tight seal was not factored into the original design calculations. Nevertheless, the increase in diameter of 1.23 mm when folded closely aligns with design anticipations. Thus, this indicates that the diameter of the millirobot could decrease by carefully aligning the middle, ensuring no overlap and minimal excess resin. The largest error percentage, a 67.88 percent deviation, was noted when the millirobot was folded, as shown by the folding difficulties depicted in Fig. 8(c). This issue, primarily due to the excess resin at the bonded seam, restricted proper folding. Future iterations will focus on refining the bonding process to avoid such complications. While a more elastic material could be used, the Elastic 50A Resin V2 showed great promise and will be used in future millirobot versions. Despite these fabrication challenges, the ability of the millirobot to compress to much less than 50 percent of its deployed size is considered a success. With improvements in the accuracy of the fabrication process, it is anticipated that the millirobot will achieve better performance and efficiency.

5. CONCLUSION

A novel deployable tensegrity millirobot for next-generation gastrointestinal diagnostics is designed and fabricated on the millimeter scale. The fabricated millirobot is 34.37 mm long, with a diameter of 12.69 mm, and can be compressed to 41.51 percent of its deployed length. Using tighter tolerances during fabrication will allow the deployable tensegrity robots to have a higher folding ratio and efficiency. In future work, the robot will be fabricated with a smaller diameter and SMA actuators will be incorporated in the active cables, allowing for minimally invasive operation.

ACKNOWLEDGEMENTS

The authors acknowledge supports from the US NSF (National Science Foundation) through grant 2104237, the NSF Graduate Research Fellowship Program awarded to Christian Kazoleas, and the American Heart Association through AHA's Second Century Early Faculty Independence Award 24SCEFIA1259736 (https://doi.org/10.58275/AHA.24SCEFIA1259736.pc.gr.193967).

REFERENCES

[1] M. Nazmul Huda, Hongnian Yu, Shuang Cang, Robots for minimally invasive diagnosis and intervention, Robotics and Computer-Integrated Manufacturing, Volume 41, 2016, Pages 127-144

[2] M. K. Goenka, S. Majumder, and U. Goenka, Capsule endoscopy: Present status and future expectation, World J. Gastroenterol., vol. 20, pp. 10024–10037, Aug. 2014.

[3] Goffredo, Rosa & Pecora, Alessandro & Maiolo, Luca & Ferrone, Andrea & Guglielmelli, Eugenio & Accoto, Dino, A Swallowable Smart Pill for Local Drug Delivery. Journal of Microelectromechanical Systems. 25. 1-9, 2016.

[4] Moglia, A., Menciassi, A., Dario, P. et al. Capsule endoscopy: progress update and challenges ahead. Nat Rev Gastroenterol Hepatol 6, 353–361, 2009.

[5] R.Goffredo, D.Accoto, and E.Guglielmelli, "Swallowable smart pills for local drug delivery: Present status and future perspectives, Expert Rev .Med. Devices, vol.12,no.5,pp.585–599,2015.

[6] Son, D., Ugurlu, M.C. and Sitti, M., 2021. Permanent magnet array–driven navigation of wireless millirobots inside soft tissues. Science Advances, 7(43), p.eabi8932.

[7] Yang, L., Zhang, T., Tan, R., Yang, X., Guo, D., Feng, Y., Ren, H., Tang, Y., Shang, W. and Shen, Y., 2022. Functionalized Spiral-Rolling Millirobot for Upstream Swimming in Blood Vessel. Advanced Science, 9(16), p.2200342.

[8] Becker, A.T., Felfoul, O. and Dupont, P.E., 2015, May. Toward tissue penetration by MRI-powered millirobots using a self-assembled Gauss gun. In 2015 IEEE International Conference on Robotics and Automation (ICRA) (pp. 1184-1189). IEEE.

[9] Erin, O., Antonelli, D., Tiryaki, M.E. and Sitti, M., 2020, May. Towards 5-dof control of an untethered magnetic millirobot via mri gradient coils. In 2020 IEEE International Conference on Robotics and Automation (ICRA) (pp. 6551-6557). IEEE.

[10] Al Khatib, E., Bhattacharjee, A., Razzaghi, P., Rogowski, L.W., Kim, M.J. and Hurmuzlu, Y., 2020. Magnetically actuated simple millirobots for complex navigation and modular assembly. IEEE Robotics and Automation Letters, 5(2), pp.2958-2965.
[11] Han, M., Guo, X., Chen, X., Liang, C., Zhao, H., Zhang, Q., Bai, W., Zhang, F., Wei, H., Wu, C. and Cui, Q., 2022. Submillimeter-scale multimaterial terrestrial robots. Science Robotics, 7(66), p.eabn0602.
[12] Zhakypov, Z., Mori, K., Hosoda, K. and Paik, J., 2019. Designing minimal and scalable insect-inspired multi-locomotion millirobots. Nature, 571(7765), pp.381-386.
[13] Haldane, D.W., Casarez, C.S., Karras, J.T., Lee, J., Li, C., Pullin, A.O., Schaler, E.W., Yun, D., Ota, H., Javey, A. and Fearing, R.S., 2015. Integrated manufacture of exoskeletons and sensing structures for folded millirobots. Journal of Mechanisms and Robotics, 7(2), p.021011.
[14] Eshaghi, K., Li, Y., Kashino, Z., Nejat, G. and Benhabib, B., 2020. mROBerTO 2.0–An autonomous millirobot with enhanced locomotion for swarm robotics. IEEE Robotics and Automation Letters, 5(2), pp.962-969.
[15] Yuan, S., and Jing, W., 2021, "Optimal Shape Adjustment of Large High-Precision Cable Network Structures," AIAA Journal, 59(4), pp. 1441-1456.
[16] Miyashita, S., Guitron, S., Ludersdorfer, M., Sung, C. R., and Rus, D., "An untethered miniature origami robot that self-folds, walks, swims, and degrades," Proc. 2015 IEEE International Conference on Robotics and Automation (ICRA), IEEE, pp. 1490-1496
[17] Shibata, M., Saijyo, F., and Hirai, S., "Crawling by body deformation of tensegrity structure robots," Proc. 2009 IEEE international conference on robotics and automation, IEEE, pp. 4375-4380.
[18] Qi Yang, Xinyu Liu, Panfeng Wang, Yimin Song, Tao Sun, A multi-locomotion clustered tensegrity mobile robot with fewer actuators, Robotics and Autonomous Systems, Volume 168, 2023.
[19] Bruce, J., Caluwaerts, K., Iscen, A., Sabelhaus, A. P., and SunSpiral, V., "Design and evolution of a modular tensegrity robot platform," Proc. 2014 IEEE International Conference on Robotics and Automation (ICRA), IEEE, pp. 3483-3489.
[20] Sabelhaus, A. P., Bruce, J., Caluwaerts, K., Manovi, P., Firoozi, R. F., Dobi, S., Agogino, A. M., and SunSpiral, V., "System design and locomotion of SUPERball, an untethered tensegrity robot," Proc. 2015 IEEE international conference on robotics and automation (ICRA), IEEE, pp. 2867-2873.
[21] Mirletz, B. T., Bhandal, P., Adams, R. D., Agogino, A. K., Quinn, R. D., and SunSpiral, V., 2015, "Goal-directed cpg-based control for tensegrity spines with many degrees of freedom traversing irregular terrain," Soft Robotics, 2(4), pp. 165-176.
[22] Friesen, J., Pogue, A., Bewley, T., de Oliveira, M., Skelton, R., and Sunspiral, V., "DuCTT: A tensegrity robot for exploring duct systems," Proc. 2014 IEEE International Conference on Robotics and Automation (ICRA), IEEE, pp. 4222-4228.
[23] Friesen, J. M., Glick, P., Fanton, M., Manovi, P., Xydes, A., Bewley, T., and Sunspiral, V., "The second generation prototype of a duct climbing tensegrity robot, DuCTTv2," Proc. 2016 IEEE International Conference on Robotics and Automation (ICRA), IEEE, pp. 2123-2128.
[24] Lessard, S., Castro, D., Asper, W., Chopra, S. D., BaltaxeAdmony, L. B., Teodorescu, M., SunSpiral, V., and Agogino, A., "A bio-inspired tensegrity manipulator with multi-DOF, structurally compliant joints," Proc. 2016 IEEE/RSJ International Conference on Intelligent Robots and Systems (IROS), IEEE, pp. 5515-5520.
[25] Schek, H.J., 1974. The force density method for form finding and computation of general networks. Computer methods in applied mechanics and engineering, 3(1), pp.115-134.
[26] Yuan, S. and Zhu, W., 2023. A Cartesian spatial discretization method for nonlinear dynamic modeling and vibration analysis of tensegrity structures. International Journal of Solids and Structures, 270, p.112179.
[27] Barnes, D. R., 1999, "Tensegrity Structures: Form, Stability, and Symmetry," Mathematics and Mechanics of Solids, 4(4), pp. 389-409
[28] Yuan, S., and Yang, B., 2019, "The fixed nodal position method for form finding of high-precision lightweight truss structures," International journal of Solids and Structures, 161, pp. 82-95.
[29] Yuan, S., and Zhu, W., 2021, "Optimal self-stress determination of tensegrity structures," Engineering Structures, 238, p. 112003.
[30] Yuan, S., Jing, W., and Jiang, H., "A Deployable Tensegrity Microrobot for Minimally Invasive Interventions," Proc. ASME International Mechanical Engineering Congress and Exposition, American Society of Mechanical Engineers, p. V005T005A061.
[31] Kazoleas, C., Mehta, K. and Yuan, S., Prototype Design and Manufacture of a Deployable Tensegrity Microrobot. IMECE Vol. 86649, ASME, 2022